



A LETTERS JOURNAL EXPLORING
THE FRONTIERS OF PHYSICS

OFFPRINT

**Estimating the strength of genuine and
random correlations in non-stationary
multivariate time series**

M. MÜLLER, G. BAIER, C. RUMMEL and K. SCHINDLER

EPL, 84 (2008) 10009

Please visit the new website
www.epljournal.org

TAKE A LOOK AT THE NEW EPL

Europhysics Letters (EPL) has a new online home at
www.epljournal.org



Take a look for the latest journal news and information on:

- reading the latest articles, free!
- receiving free e-mail alerts
- submitting your work to EPL

www.epljournal.org

Estimating the strength of genuine and random correlations in non-stationary multivariate time series

M. MÜLLER^{1,2(a)}, G. BAIER^{1,3}, C. RUMMEL^{4,1} and K. SCHINDLER⁴

¹ *Facultad de Ciencias, Universidad Autónoma del Estado de Morelos - 62209 Cuernavaca, México*

² *Max-Planck-Institut für Physik komplexer Systeme - D-01187 Dresden, Germany, EU*

³ *Manchester Interdisciplinary Biocentre, University of Manchester - Manchester M1 7DN, UK, EU*

⁴ *Department of Neurology, Inselspital, Bern University Hospital, and University of Bern - Switzerland*

received 4 June 2008; accepted in final form 25 August 2008

published online 19 September 2008

PACS 05.45.Tp – Time series analysis

PACS 89.75.Fb – Structures and organization in complex systems

PACS 87.19.L- – Neuroscience

Abstract – The estimation of the amount of genuine cross-correlation strength from multivariate data sets is a nontrivial task, especially when the power spectra of the signals vary dynamically. In this case, the amount of random correlations may vary drastically, even when the length T of the data window used for the construction of the zero-lag correlation matrix is kept constant. In the present letter we introduce correlation measures that allow to distinguish quantitatively genuine and random cross-correlations. The measures are carefully tested by employing model data and exemplarily we demonstrate their performance by their application to a clinical electroencephalogram (EEG) of an epilepsy patient.

Copyright © EPLA, 2008

Introduction. – Any statistical measure that, in a strict mathematical sense, is defined via an integral over an infinite range yields only imperfect estimates of the desired quantity when calculated over a finite data window. When linear cross-correlations are considered, this fact is manifested by the appearance of random correlations [1]. If one calculates the Pearson coefficient for two uncorrelated signals registered with given sampling frequency over a finite range of T data points, the result is not necessarily zero. Instead, nonzero values appear in accordance to a symmetric, bell-shaped distribution function centered around zero. The width of this function is determined by the length T of the data window and tends to zero if $T \rightarrow \infty$. However, also the frequency contents of the signals, *i.e.* their power spectra have a major influence on the results. If one understands the correlation coefficient as an average over the product of two time series, it is clear, that this averaging procedure works less effective if the period of the slowest dominant frequencies gets larger. Hence, for any finite T , the width of the distribution, and therefore the probability for the occurrence of large correlation coefficients, gets larger with increasing power of low frequencies relative to fast components.

Recently, techniques known from Random Matrix Theory (RMT) have been introduced in order to separate random from genuine cross-correlations in multivariate data sets [2,3]. In contrast to the former the latter indeed allow for conclusions on genuine interrelations between different data channels. It results that those parts of the spectrum of eigenvalues and eigenvectors of the zero-lag cross-correlation matrix, which are dominated by random correlations and noise follow the universal behavior of the random matrix ensembles, while otherwise deviations from the universal RMT-predictions could be observed.

Genuine cross-correlations provoke nonrandom repulsions between certain eigenvalues [4], which might occur at any location along the eigenvalue spectrum, *i.e.* in the central part as well as at both edges. Which eigenvalues are affected by such nonrandom repulsions depends on the correlation structure of the multivariate data set [5], *i.e.* it is determined by the correlation scheme between the data channels (cliques, trees, chains, etc.). Eigenvalues that are not affected by such repulsions, the “bulk” of eigenvalues, are randomly distributed around 1, where the width of this distribution is uniquely determined by the amount of random correlations and noise. In this way, any specific correlation structure within a multivariate data set leads to a particular repulsion scheme of the eigenvalues [5,6].

^(a) E-mail: muellerm@buzon.uaem.mx

Hence, an increase of (random as well as genuine) cross-correlations leads in general to a broadening of the eigenvalue distribution, while for less correlated data the eigenvalues get more closely distributed around unity. Consequently, if one only intends to estimate the average strength of total correlations it suffices to consider the width of the eigenvalue distribution. In fact, the time evolution of the largest eigenvalue gives already a fair estimate for this quantity [1].

However, if one aims to characterize dynamical changes of the genuine cross-correlation structure via a moving window approach this strategy may fail if the frequency content of the signals also varies, as *e.g.* for electroencephalograms (EEG). Here, the power spectra of the signals may vary significantly with time, for example during states of different grades of vigilance like wakefulness and sleep, or specifically during pathological conditions, as *e.g.* an epileptic seizure. Then, the relative amount of random and genuine correlation may alter drastically, even when all-parameters of the analysis method are kept constant. In such cases, a quantitative distinction between genuine cross-correlations and random contributions is a nontrivial task and to the best of our knowledge an all-purpose formalism for multivariate data sets is missing so far.

Methods. –

The zero-lag cross-correlation matrix. An M -dimensional multivariate data set of length T can be written as the $M \times T$ data matrix \mathbf{X} . In this notation, the zero-lag cross-correlation matrix \mathbf{C} is given as $\mathbf{C} = \frac{1}{T} \mathbf{X} \mathbf{X}^t$, where it is assumed, that each of the M time series is normalized to zero mean and unit variance. As \mathbf{C} is real and symmetric it has real eigenvalues λ_i and eigenvectors $\vec{v}_i : \mathbf{C} \vec{v}_i = \lambda_i \vec{v}_i$. Here the eigenvalues are denoted in increasing order $\lambda_i \leq \lambda_{i+1}$. As the diagonal elements of \mathbf{C} are all equal to one, the trace of \mathbf{C} is equal to M , the dimension of the data set: $\text{Tr } \mathbf{C} = \sum_{i=1}^M C_{ii} = \sum_{i=1}^M \lambda_i = M$, which means that the change of any eigenvalue λ_i has to be compensated by a corresponding change of some of the others, such that the sum stays constant.

Surrogate data as a means to estimate the strength of genuine cross-correlation. For testing the null-hypothesis of zero genuine cross-correlations one needs to create artificial time series where true relationships between different data channels are destroyed while linear univariate properties like the auto-correlation functions are conserved. If the zero-lag correlation matrix is then constructed from this data, the resulting eigenvalue spectrum serves to test for the null hypothesis of zero genuine cross-correlations. In general this can be achieved by amplitude adjusted Fourier-based surrogates [7], a strategy, which is followed in this paper. All surrogate data used in this publication were generated by the freely available TISEAN software package [8,9].

While the distribution of eigenvalues computed from surrogates λ_i^s reflects purely random cross-correlations,

the eigenvalue spectra obtained from the original data λ_i represent a mixture of both, random as well as genuine contributions. Hence, any significant deviation of the eigenvalues λ_i from λ_i^s indicates the presence of genuine cross-correlations. On the basis of these considerations we define a quantity that measures the genuine cross-correlation strength (CCS) within the data set as

$$\text{CCS} = \frac{\sum_{i=1}^M \Lambda_i}{\sum_{i=1}^{M-1} \bar{\lambda}_i^s + (M - \bar{\lambda}_M^s)} \quad (1)$$

with

$$\Lambda_i = \begin{cases} |\bar{\lambda}_i - \bar{\lambda}_i^s| \Theta(\bar{\lambda}_i - \Delta_i - (\bar{\lambda}_i^s + \Delta_i^s)), & \text{if } \bar{\lambda}_i > \bar{\lambda}_i^s, \\ |\bar{\lambda}_i - \bar{\lambda}_i^s| \Theta(\bar{\lambda}_i^s - \Delta_i^s - (\bar{\lambda}_i + \Delta_i)), & \text{if } \bar{\lambda}_i \leq \bar{\lambda}_i^s. \end{cases} \quad (2)$$

Here $\Theta(x)$ is the step function with $\Theta(x) = 0$ if $x \leq 0$ and $\Theta(x) = 1$, otherwise. Δ_i (Δ_i^s) denote the standard deviation and $\bar{\lambda}_i$ ($\bar{\lambda}_i^s$) the average eigenvalues calculated from the original data and the surrogates, respectively. The averages are taken over an ensemble of correlation matrices which might be constructed over a certain data segment. The denominator of (1) ensures that the CCS-coefficient varies between zero and one, which can be easily seen by the consideration of two limiting cases. If no genuine cross-correlations are present, the eigenvalues calculated from the original data are (besides statistical fluctuations) equal to those calculated from the surrogates and the sum of the numerator equals zero. If, on the other hand, all time series are identical, the largest eigenvalue $\lambda_M = M$, while all others are identical to zero. In that case, numerator and denominator of eq. (1) are identical and in consequence $\text{CCS} = 1$. Note, the quantity (1) measures significant deviations of the eigenvalues along the whole spectrum and is therefore sensitive to detect any kind of correlation pattern within the multivariate data set.

In a similar manner one can define coefficients, which measure the total correlation strength (TCS) as well as the amount of the random correlations (RCS):

$$\text{TCS} = \frac{\sum_{i=1}^M |1 - \bar{\lambda}_i|}{2M - 2}, \quad (3)$$

$$\text{RCS} = \frac{\sum_{i=1}^M |1 - \bar{\lambda}_i^s|}{2M - 2}. \quad (4)$$

Here, the deviations of the corresponding average eigenvalues from unity (the case for completely uncorrelated data in the limit $T \rightarrow \infty$) are measured and normalized by its sum for the case of identical data channels.

A simple test-framework. We aim to test whether CCS is capable of detecting changes in the amount of genuine cross-correlations independently of changes of the auto-correlation lengths of the signals. Simultaneously we test whether RCS correctly detects dynamical changes of the amount of random correlations. To this end, we use

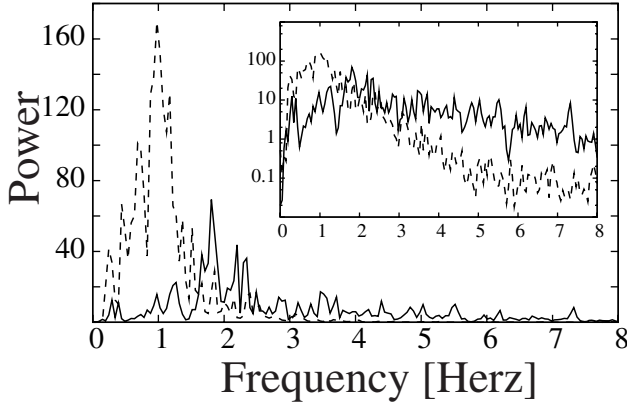


Fig. 1: Power spectrum of the seizure period (solid line) and of the immediate post-seizure period (dashed line) of electrode F3. The inlet shows the same power spectra in logarithmic scale.

a simple model that allows to control separately genuine cross-correlations as well as the power spectra of the data channels. A multivariate data set is created as a superposition of harmonic oscillators known as N_f -tori, see e.g. [5]:

$$X_i(t) = \sum_{s=1}^{N_f} A_{is} \sin(2\pi f_s t + \delta_{is}), \quad i = 1, \dots, M. \quad (5)$$

The randomly chosen frequencies f_s are the same for all data channels. Via the distribution of the amplitudes A_{is} the power spectra of the $X_i(t)$ can be adjusted, while the distribution of the partial phases δ_{is} determines the phase relationships between the data channels. If the δ_{is} are uniformly distributed between zero and 2π the signals $X_i(t)$ are mutually uncorrelated in the ensemble average. (Note, the distribution of a finite number N_f of δ_{is} is not strictly uniform. Hence, some possibly small genuine correlations are induced, which are, however, vanishing by considering an ensemble of such trials or by increasing N_f .) Otherwise phase correlations are present. As in this letter we apply the method to EEG data of an epilepsy patient we adapt the amplitudes in accordance with the power spectra of a typical scalp recording of a focal onset seizure, although the model (5) can be fitted to any other experimental multivariate data set. The adjustment of the amplitudes A_{is} to power spectra of experimental data has the additional advantage that the time unit of the artificially created data is well defined. We consider $N_f = 5000$ frequencies and as we focus on a standard surface EEG-recording we create $M = 19$ data channels in all cases. Power spectra, computed from different epochs of an experimental EEG-recording are used: The power spectra of the M channels of a seizure epoch and those of the immediate post-seizure period (see fig. 1). The difference between these power spectra is that during the seizure, small frequency components with $f \leq 1$ Hz are considerably suppressed while it shows a fat tail towards large frequency components. On the contrary, in the

post-seizure period fast components are diminished and dominant contributions between 0.1 and 1.5 Hz can be measured.

On this basis, we create data sets which are divided in three segments. Segment I lasts from second 0 to 95 and segment III from second 105 to 200. Either the amplitude or the phase distribution are different between these two segments. The transitional segment II, defined between second 95 to 105, is used to shift either the A_{is} and/or the δ_{is} linearly between the values defined by the distributions of the two adjacent segments. Three different cases are considered:

1. Model A

The amplitudes A_{is} are kept constant over the whole time course and resemble the power spectra of an EEG during the period of a typical epileptic focal onset seizure. The phases δ_{is} of segment I are chosen such that two correlation clusters, each containing four data channels are formed. For $X_i(t)$, $i = 1, \dots, 4$ the δ_{is} are Gaussian distributed (modulo 2π) centered at $3/4\pi$ and with a standard deviation $\pi/4$. For $X_i(t)$, $i = 5, \dots, 8$ a Gaussian distribution with the same width but centered at $5/4\pi$ is used. In this way both groups are basically uncorrelated. The remaining data channels are uncorrelated (on the ensemble average). In segment III, the phases δ_{is} are randomly chosen due to a uniform distribution such that all data channels get uncorrelated during the transitional segment II.

2. Model B

The phases δ_{is} of all data channels are uniformly distributed between zero and 2π over the whole time course. The amplitudes A_{is} of segment I are adjusted to the power spectra of the seizure epoch, while they are chosen in accordance to the power spectra of the immediate post-seizure period for segment III.

3. Model C

Segment I is chosen with identical parameters as the first segment of model A while segment III is equivalent to the last segment of model B.

From the time series created by these models, intervals of 1000 data points (equivalent to 5 seconds) are defined and shifted with a step size of 250 sampling points along the recording. For each interval, 20 Fourier based surrogates are computed. Then, we analyze the intervals of the original data as well as those of the surrogates. For this purpose we construct the zero-lag correlation matrix over a window of $T = 500$ data points (corresponding to 2.5 seconds), which is then shifted with a step width of 40 data points (0.2 seconds) along the interval. In this way, we obtain an ensemble of 13 correlation matrices for the original data and another ensemble of 260 matrices for the surrogates. These matrices are diagonalized and ensemble averaged eigenvalues $\bar{\lambda}_i$ and $\bar{\lambda}_i^s$ (and the respective standard deviations) are obtained for each interval, which are

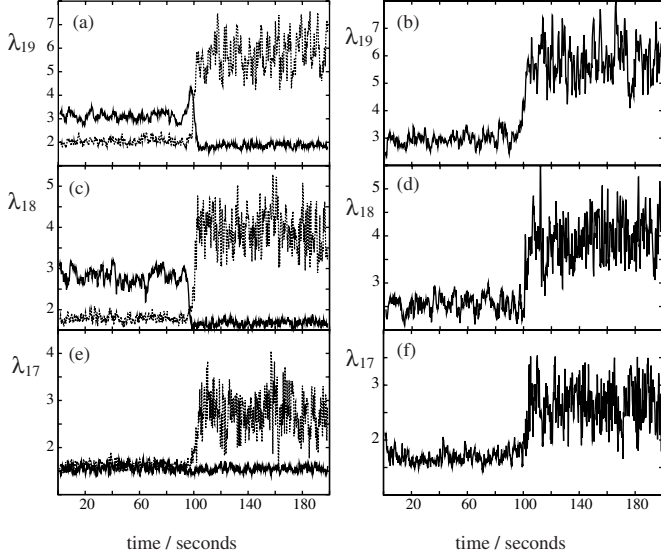


Fig. 2: The three largest average eigenvalues as a function of time calculated for model A (solid line of panels (a), (c) and (e)), model B (dashed line of panels (a), (c) and (e)) and model C (panels (b), (d) and (f)).

then used to compute the correlation measures (1), (3) and (4).

Results. –

Model data. When two groups, each of them containing m_k data channels, are formed two elevated eigenvalues at the upper edge and for each group $m_k - 1$ decreased eigenvalues at the lower edge of the eigenvalue spectrum are expected [5]. Therefore, in the case of model A and C one could expect two elevated eigenvalues at the upper edge during the first time segment which approach the bulk region during the transient segment II. The behavior of the three largest eigenvalues obtained by analyzing the data computed by model A, B and C is summarized in fig. 2.

If the power spectra do not change, the evolution of the eigenvalues fits to the expectation. $\bar{\lambda}_{19}$ and $\bar{\lambda}_{18}$ show elevated values during the first segment, where two mutually independent correlation clusters are formed. Then, during the short transient segment II they move back and approach the bulk. The third largest eigenvalue $\bar{\lambda}_{17}$ stays unaffected by the changes of the correlation structure. It fluctuates over the whole time course around some average value. On the contrary, for model B, where solely the power spectra are varied, the three largest eigenvalues (and some of the next largest ones) increase drastically when passing to segment III. Such a behavior could be interpreted as an increase of genuine cross-correlations during the transient segment II [5]. The same is true for model C. Also here, a pronounced increase of the largest eigenvalues can be observed, when passing to segment III. The de-correlation of the two clusters is completely overshadowed by the change of the power spectra. This illustrates clearly, that the eigenvalue distribution is sensitive

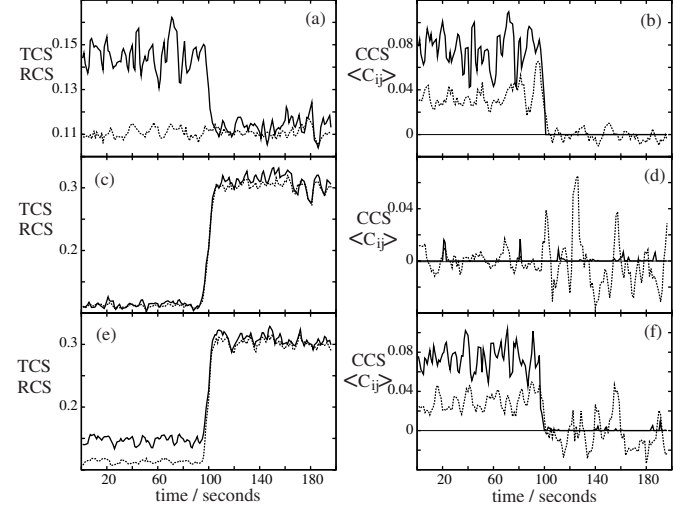


Fig. 3: TCS (solid line) and RCS (dashed line) of model A (a), model B (c) and model C (e). CCS (solid line) and average non-diagonal element of the zero-lag cross-correlation matrix (dashed line) for model A (b), model B (d) and model C (f).

to changes of the autocorrelation times of the signals. If this influence is not taken into account, inspecting the eigenvalues would lead to erroneous interpretation of the results.

Next we turn to the evaluation of the correlation measures defined above. Figure 3 shows the development of measures (1), (3) and (4) for the same model data as discussed in the previous figure. Furthermore the time course of the average non-diagonal element of the zero-lag cross-correlation matrix is drawn for comparison. When the power spectra are not altered between the segments, the amount of random correlations stays constant on the average. Hence, for model A it is expected that RCS shows the behavior as indicated by the dashed line of fig. 2a, *i.e.* it fluctuates around some constant value over the whole time course. For the total as well as the genuine cross-correlation strength the situation is different. As the two correlation clusters fade during the transient segment II, both values, CCS as well as TCS should decrease significantly within this period. Figures 3a and b demonstrate that TCS decreases to the mean value of RCS during the uncorrelated last segment, while CCS decreases strictly to zero when the correlations are diminished. The average non diagonal element of \mathbf{C} shows qualitatively a similar behavior as CCS. On the average $\langle C_{ij} \rangle$ decreases also to zero with vanishing genuine correlations. However, fig. 3b shows clearly, that the relative fluctuations of the $\langle C_{ij} \rangle$ are considerably larger than those of CCS (in fact CCS does not fluctuate in segment III) and hence, the results for the average correlation coefficient is less significant.

The same is observed, when analysing data of model B. As this model does not generate any genuine cross-correlations, one would expect zero or small values, both for CCS as well as for $\langle C_{ij} \rangle$. Qualitatively this

expectation is confirmed by fig. 3d CCS shows only a few small deviations from zero over the whole time course. On the contrary, $\langle C_{ij} \rangle$ fluctuates irregularly around zero with considerable amplitude. These fluctuations increase drastically during segment III, where a larger contribution of slow frequency components causes an increase of random correlations. On the other hand, due to the lack of genuine cross-correlations TCS and RCS shows qualitatively the same behavior for Model B.

Finally, the results obtained for model C are shown in figs. 3e and f. TCS is slightly larger than RCS during segment I, which is due to the genuine cross-correlations of the two correlation clusters. Then, during segment III, both quantities are uniquely governed by random correlations and hence, take almost the same values. CCS, on the other hand, clearly detects the genuine correlations of segment I and decreases to zero almost everywhere during segment III. When considering $\langle C_{ij} \rangle$, it is much more difficult to distinguish the uncorrelated from the correlated segment. The simultaneous changes of the power spectrum strongly impair the discriminative potency of this quantity. As in the case of model A (fig. 3b) it fluctuates at some lower value during segment I. Due to the considerably larger fluctuations during segment III, the changes of $\langle C_{ij} \rangle$ are marginal compared to those observed for the CCS-coefficient.

Application to real world data: Illustration of an exemplary case. Finally we show exemplarily the application of the data set. In the present case, we consider the electroencephalographic scalp recording (EEG) of a 22 year old male patient, who suffered from refractory partial epilepsy with temporal lobe seizures and took part in the local program for presurgical evaluation of the Department of Neurology of the Inselspital of the University of Bern. Seizure onsets and seizure endings were assessed by an experienced epileptologist and electroencephalographer (KS).

We selected from a long-term recording one piece of 1500 seconds duration, such that the seizure starts at second 600. In order to avoid a dominant influence of large amplitudes we normalized the data channels separately to zero mean and unit variance. To this end we used a data window containing 1000 data points, which was shifted with a maximal overlap over the recordings. Then we transformed the EEG recording to the global average reference as this specific montage turns out to distort the eigenvalue spectrum least [10]. Essentially, only the smallest eigenvalue is affected by this reference. Therefore we excluded $\bar{\lambda}_1$ from the analysis. However, the normalization and the particular choice of the reference is by no means essential. In fact, we checked their performance by using different reference schemes (with and without normalization) obtaining qualitatively similar results. Furthermore we emphasize, that the application of (1), (3) and (4) is *not* restricted to EEG data only.

Similar to the analysis of the data derived from the N_f -tori (5) we divided the recording into intervals of

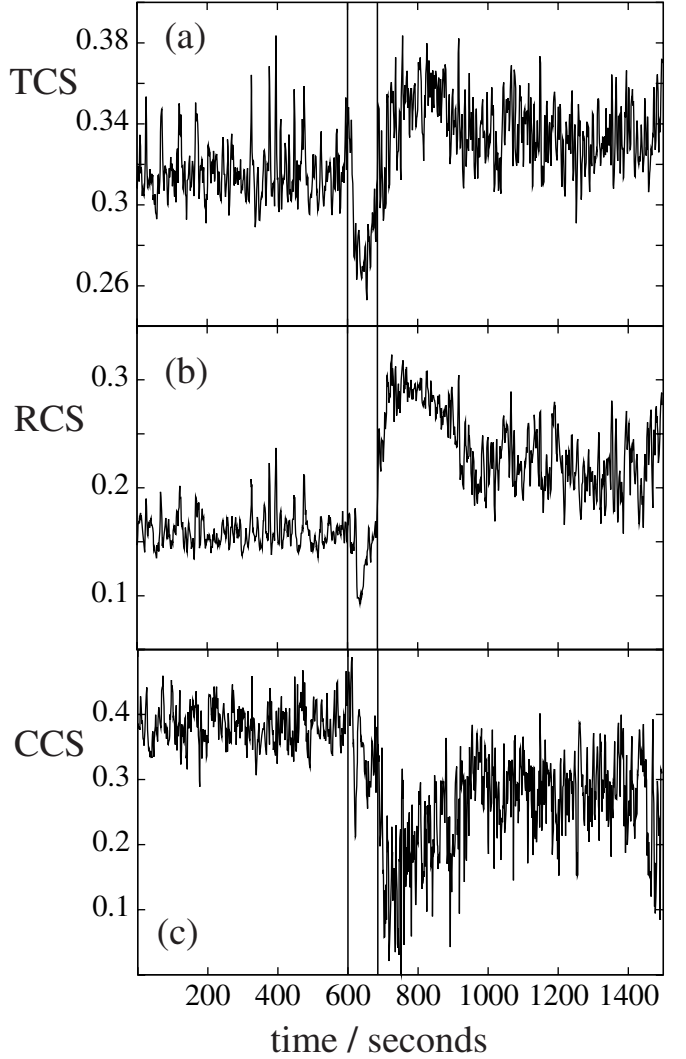


Fig. 4: TCS (a), RCS (b) and CCS (c) calculated from clinical EEG recordings of an epilepsy patient. Seizure onset and offset are indicated by thick vertical lines.

length 1000, which were displaced by a step width of 250 data points along the time series. Analysis of these intervals was performed as described above. The results are summarized in fig. 4. All three quantities, TCS (fig. 4a), RCS (fig. 4b) and CCS (fig. 4c) are fluctuating around some constant value during the 10 minutes before seizure onset. Then, during the seizure, a significant decrease of the total correlation strength can be measured, which is followed by a considerable increase during the immediate post-seizure period [11]. The same is true for the RCS-value. Although the decrease during the seizure is less pronounced than that of TCS, its relative increase just at seizure offset is larger. It increases roughly to twice the average of its pre-seizure value. Only a few minutes after seizure offset, around second 1000, it saturates to a value slightly above that of the pre-seizure state.

The genuine cross-correlation strength on the other hand shows a qualitatively different picture. A certain correlation loss during the seizure can be measured, but

now this declining tendency continues and it encounters a pronounced minimum after seizure offset at almost the same time where TCS and RCS show maximal values. After that, it increases gradually and saturates at about 1000 seconds.

Discussion and conclusions. – The correlation measures (1), (3) and (4) are able to extract different properties from a multivariate data set. TCS measures essentially the widths of the eigenvalue distribution and is therefore a direct measure for the total amount of cross-correlations within a multivariate recording (figs. 3a, c and e). When the amount of random correlations stays constant over the whole time course, the dynamical changes of TCS reflect the evolution of the genuine cross-correlations (fig. 3a). In this case, the average correlation coefficient as well as the evolution of the largest eigenvalue give already a fair measure for the genuine cross-correlation strength [1] although with large fluctuations. RCS, on the other hand, measures the widths of the eigenvalue spectrum derived from surrogate data, where all genuine cross-correlations are destroyed on the ensemble average. Hence, if the eigenvalues are averaged over a set of surrogates, RCS is exclusively affected by the amount of random correlations. If the power spectra of a complex system vary with time, also the amount of random correlations alters (fig. 3c). In this case it is a difficult task to estimate the time varying random contributions from the original recordings alone. A direct inspection of the evolution of the eigenvalues might lead to erroneous conclusions (figs. 2a, c and e). Figures 3 and 4 demonstrate, that CCS extracts nicely the amount of genuine cross-correlations.

In [12] thresholding was applied to the zero-lag cross-correlation matrix in order to identify correlation clusters, implicitly assuming, that genuine cross-correlations generate larger entries in \mathbf{C} than random correlations and noise. The time dependence of the cross-correlation strength was characterized by the means of a few largest and smallest eigenvalues, respectively, in [13]. In [14] correlation clusters of *in vitro* recordings of epileptic seizures in rats were studied using the participation index [15]. A measure for the strength of cross-correlations within a cluster was proposed on the basis of the eigenvalues of \mathbf{C} derived from surrogate data. However, no clear distinction between the overall strength of genuine and random cross-correlations was made.

In principle, a simple average over the nondiagonal elements of \mathbf{C} should lead to similar results as CCS. Random correlations lead to a symmetric, bell-shaped distribution of the C_{ij} around zero because positive and negative entries appear with the same probability, while genuine correlations lead in general to some kind of asymmetric distribution function. Therefore, on the average random contributions should vanish. However, as documented in fig. 3b, d and f, this averaging process performs less effective (especially for small M) than the filtering provided by the CCS-coefficient, which occurs in principle in two steps. First, due to the Heaviside

function $\Theta(x)$ in the definition of (1) the whole bulk part of the spectrum, which is uniquely affected by random correlations, is excluded. Second, the overall broadening of the eigenvalue spectrum provoked by (changes of) the frequency content of the signals is taken into account by comparing the eigenvalues of the original spectrum with those derived from the surrogates. For this reason, CCS suffers less from statistical fluctuations than, *e.g.* $\langle C_{ij} \rangle$, where all contributions enter directly.

In general no assumptions about specific correlation patterns, as, *e.g.* that genuine contributions in \mathbf{C} provoke larger absolute values than random correlations, are made. The measures (1), (3) and (4) capture the strength of genuine cross-correlations independently of variations of the power spectra and independently of the repulsion scheme of the eigenvalues making CCS and RCS powerful tools for the analysis of non-stationary multivariate signals.

This work was supported by Deutsche Forschungsgemeinschaft, Germany (grant RU1401/1-2), Novartis Jubiläumsstiftung, Switzerland and CONACyT, Mexico (Proj. No. 48500).

REFERENCES

- [1] PLEROU V., GOPIKRISHNAN P., ROSENOW B., NUNES AMARAL L. A., GUHR T. and STANLEY H. E., *Phys. Rev. E*, **65** (2002) 066126.
- [2] LALOUX L., CIZEAU P., BOUCHAUD J.-P. and POTTERS M., *Phys. Rev. Lett.*, **83** (1999) 1467.
- [3] PLEROU V., GOPIKRISHNAN P., ROSENOW B., NUNES AMARAL L. A. and STANLEY H. E., *Phys. Rev. Lett.*, **83** (1999) 1471.
- [4] UTSUGI A., INO K. and OSHIKAWA M., *Phys. Rev. E*, **70** (2004) 026110.
- [5] MÜLLER M., BAIER G., GALK A., STEPHANI U. and MUHLE H., *Phys. Rev. E*, **71** (2005) 046116.
- [6] MÜLLER M., LÓPEZ JIMÉNEZ Y., RUMMEL C., BAIER G., GALK A., STEPHANI U. and MUHLE H., *Phys. Rev. E*, **74** (2006) 041119.
- [7] KANTZ H. and SCHREIBER T., *Nonlinear Time Series Analysis, Cambridge Nonlinear Sci. Ser.* (Cambridge University Press, Cambridge) 1997.
- [8] HEGGER R., KANTZ H. and SCHREIBER T., *Chaos*, **9** (1999) 413.
- [9] SCHREIBER T. and SCHMITZ A., *Physica D*, **142** (2000) 346.
- [10] RUMMEL C., BAIER G. and MÜLLER M., *J. Neurosci. Methods*, **166** (2007) 138.
- [11] MÜLLER M., BAIER G., RUMMEL C. and SCHINDLER K., submitted to *Clin. Neurophysiol.* (2008).
- [12] KIM D.-H. and JEONG H., *Phys. Rev. E*, **72** (2005) 046133.
- [13] SCHINDLER K., LEUNG H., ELGER C. E. and LEHNERTZ K., *Brain*, **130** (2007) 65.
- [14] LI X., CUI D., JURUSKA P., FOX J. E., YAO X. and JEFFERYS J. G. R., *J. Neurophysiol.*, **98** (2007) 3341.
- [15] ALLEFELD C., MÜLLER M. and KURTHS J., *Int. J. Bifurcat. Chaos*, **17** (2007) 3493.